

Electronic Supporting Information (ESI)

A flexible zwitterion ligand based lanthanide metal-organic framework for luminescence sensing of metal ions and small molecules

Rong-Mei Wen, Song-De Han, Guo-Jian Ren, Ze Chang, Yun-Wu Li* and Xian-He Bu*

Department of Chemistry, TKL of Metal- and Molecule-Based Material Chemistry and Synergetic Innovation Center of Chemical Science and Engineering (Tianjin), Nankai University, Tianjin 300071, P. R. China.

*Corresponding author. E-mail: liyunwu@lcu.edu.cn (Yun-Wu Li); buxh@nankai.edu.cn (Xian-He Bu). Fax: +86-22-23502458.

Experimental Section

Materials and Physical measurements.

The flexible zwitterion ligand H_3LBr_3 was prepared according to the method described in the literature.¹ Other chemicals were commercially available and used as received. IR spectra were measured on a Tensor 27 (Bruker) FT-IR spectrometer with KBr pellets. UV/Vis absorption spectra were measured with a Hitachi U-3010 UV-Vis spectrophotometer (Hitachi, Japan). The Powder X-ray diffraction (PXRD) experiments were recorded on a Bruker D8 FOCUS diffractometer with a Cu-target tube and a graphite monochromator. Simulation of the PXRD spectra were carried out by the single-crystal data and diffraction-crystal module of the Mercury (Hg) program available free of charge *via* the Internet at <http://www.iucr.org>. All fluorescence measurements were performed on a Hitachi F-4500 fluorescence spectrophotometer equipped with a plotter unit.

X-ray Data Collection and Structure Determinations.

The crystallographic data of complex were collected on a Rigaku MSC diffractometer at 293(2) K with Mo-K α radiation ($\lambda = 0.71073 \text{ \AA}$). The program *CrystalClear* was used for integration of the diffraction profiles. The crystal data were solved by direct methods and refined by a full-matrix least-square method on F^2 using the *SHELXL-97* crystallographic software package.² From the difference Fourier map of **1**, a number of diffuse scattered peaks with electron density were observed, which can be attributed to the disordered solvent molecules. Attempts to model these peaks were unsuccessful because the residual electron density peaks obtained were diffused. So PLATON/SQUEEZE³ was used to refine the structure further. Detailed crystallographic data are summarized in Table S1 and the selected bond lengths and angles are given in Tables S2. Full crystallographic data for **1** have been deposited with the CCDC (1015226). These data can be obtained free of charge from The Cambridge Crystallographic Data Centre *via* www.ccdc.cam.ac.uk/data_request/cif.

Table S1. Crystal data and structural refinements for **1**.

Formula	EuC ₃₀ H ₂₉ O ₁₁ N ₄
F _w	773.54
T/K	293(2) K
$\lambda/\text{\AA}$	0.71073
Crystal system	Triclinic
Space group	<i>P</i> -1
<i>a</i> /\AA	9.5782(19)
<i>b</i> /\AA	12.778(3)
<i>c</i> /\AA	18.945(4)
$\alpha/^\circ$	107.49(3)
$\beta/^\circ$	99.21(3)
$\gamma/^\circ$	97.89(3)
<i>V</i> /\AA ³	2140.2(8)
<i>Z</i>	2
<i>D</i> _c /Mg·cm ⁻³	1.200
μ/mm^{-1}	1.514
<i>F</i> (000)	776
total reflns	18617
unique reflns	7534
<i>R</i> _{int}	0.0742
Final <i>R</i> indices	<i>R</i> ₁ = 0.0575, <i>wR</i> ₂ = 0.1240
<i>wR</i> ₂ (all data) ^{<i>b</i>}	<i>R</i> ₁ = 0.0795, <i>wR</i> ₂ = 0.1306
GOF on <i>F</i> ²	1.032

^{*a*} $R_1 = \sum ||F_o| - |F_c|| / \sum |F_o|$. ^{*b*} $wR_2 = \{ \sum [w(F_o^2 - F_c^2)^2] / \sum w(F_o^2)^2 \}^{1/2}$

Table S2 The selected bond lengths [Å] and angles [°] of **1**.

Eu(1)-O(3)	2.343(4)	Eu(1)-O(2)#2	2.362(5)
Eu(1)-O(6)#3	2.377(4)	Eu(1)-O(4)#4	2.408(4)
Eu(1)-O(1)#1	2.436(4)	Eu(1)-O(5)#5	2.440(5)
Eu(1)-O(8)	2.446(5)	Eu(1)-O(7)	2.486(5)
O(1)-Eu(1)#1	2.436(4)	O(2)-Eu(1)#7	2.362(5)
O(4)-Eu(1)#4	2.408(4)	O(5)-Eu(1)#5	2.440(5)
O(6)-Eu(1)#8	2.377(4)	O(3)-Eu(1)-O(2)#2	145.40(19)
O(3)-Eu(1)-O(6)#3	142.88(19)	O(2)#2-Eu(1)-O(6)#3	71.65(17)
O(3)-Eu(1)-O(4)#4	100.54(15)	O(2)#2-Eu(1)-O(4)#4	81.26(17)
O(6)#3-Eu(1)-O(4)#4	78.81(16)	O(3)-Eu(1)-O(1)#1	80.41(16)
O(2)#2-Eu(1)-O(1)#1	119.21(16)	O(6)#3-Eu(1)-O(1)#1	78.47(17)
O(4)#4-Eu(1)-O(1)#1	141.94(18)	O(3)-Eu(1)-O(5)#5	80.45(16)
O(2)#2-Eu(1)-O(5)#5	79.23(17)	O(6)#3-Eu(1)-O(5)#5	121.05(15)
O(4)#4-Eu(1)-O(5)#5	145.10(18)	O(1)#1-Eu(1)-O(5)#5	72.92(17)
O(3)-Eu(1)-O(8)	73.11(18)	O(2)#2-Eu(1)-O(8)	74.21(17)
O(6)#3-Eu(1)-O(8)	139.18(18)	O(4)#4-Eu(1)-O(8)	74.47(18)
O(1)#1-Eu(1)-O(8)	139.20(18)	O(5)#5-Eu(1)-O(8)	72.51(17)
O(3)-Eu(1)-O(7)	71.54(18)	O(2)#2-Eu(1)-O(7)	139.48(18)
O(6)#3-Eu(1)-O(7)	72.87(17)	O(4)#4-Eu(1)-O(7)	73.23(18)
O(1)#1-Eu(1)-O(7)	71.10(17)	O(5)#5-Eu(1)-O(7)	137.24(18)
O(8)-Eu(1)-O(7)	125.81(17)		

Symmetry transformations used to generate equivalent atoms: #1: -x+1, -y+1, -z+2; #2: x-1, y-1, z-1; #3: x-1, y, z-1; #4: -x+1, -y, -z+1; #5: -x+1, -y, -z+2; #7: x+1, y+1, z+1; #8: x+1, y, z+1.

Synthesis and Characterization

Preparation of $[\text{EuL}(\text{OH})_2](\text{NO}_3) \cdot x(\text{solvent})$.

$[\text{EuL}(\text{OH})_2](\text{NO}_3) \cdot x(\text{solvent})$ (**1**). H_3LBr_3 (0.1 mmol) and $\text{Eu}(\text{NO}_3)_3 \cdot 6\text{H}_2\text{O}$ (0.20 mmol) were thoroughly dissolved in 9 mL solution of DMF/ H_2O / $\text{C}_2\text{H}_5\text{OH}$ ($V/V/V = 1 : 1 : 1$, DMF = *N,N'*-Dimethylformamide). Colorless crystals were obtained by slow evaporation at room temperature over 24 h. Yield: 35% based on **L**. FT-IR (KBr pellet, cm^{-1}): 3385(s), 2361(m), 1610(s), 1566(s), 1384(s), 1137(w), 1042(w), 880(s), 825(s), 798(s), 775(s), 734(w), 697(m), 559(m).

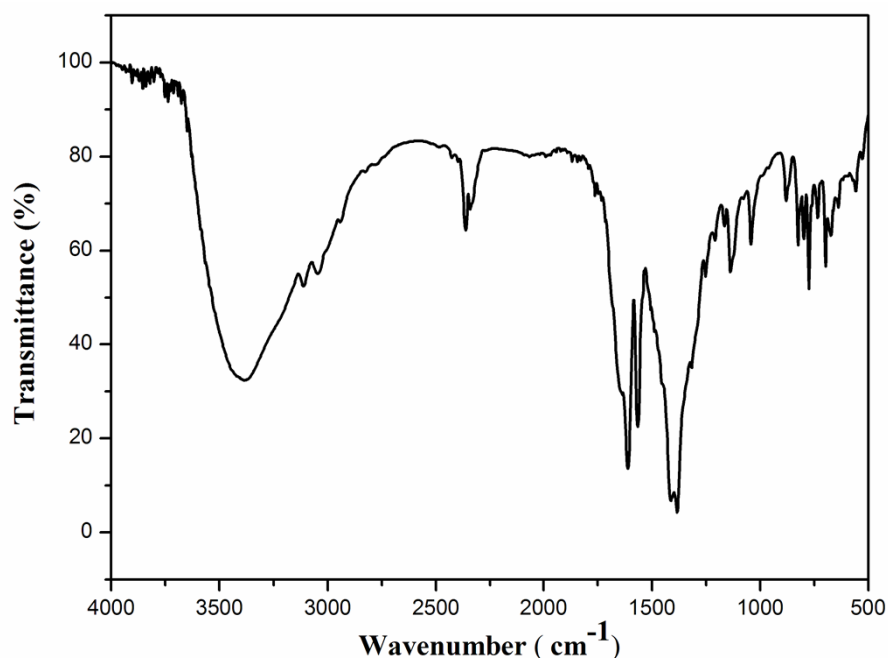


Fig. S1 FT-IR spectra of **1**.

Characterization

The PXRD experiment was performed in order to make sure that the crystal structure is truly representative of the bulk materials. Good consistence between the experimental pattern and the simulated pattern as displayed in Fig. S2 indicates that bulk-synthesized materials are homogeneous. The thermal gravimetric analysis (TGA) indicated that **1** has one onset step from 100 °C to 250 °C to breathe out the structurally disordered solvent molecules (Fig. S3). **1** was stable in common solvents and can be easily dispersed in common solvents without changing its original structure (Fig. S4).

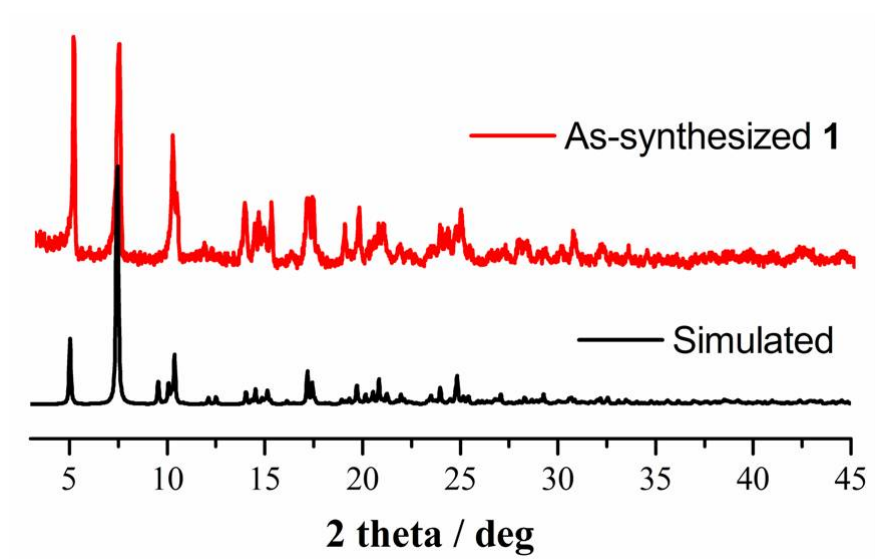


Fig. S2 The Powder X-ray diffraction pattern of **1**.

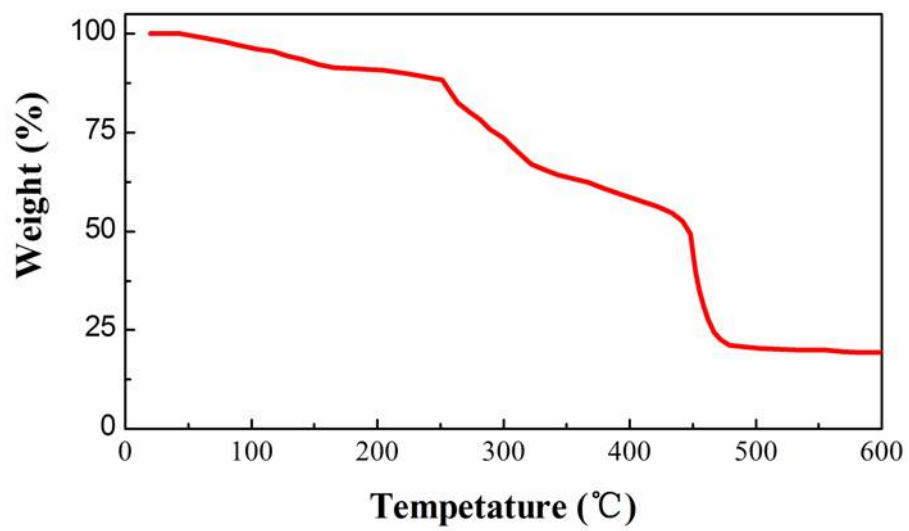


Fig. S3 The TGA diagrams of **1**.

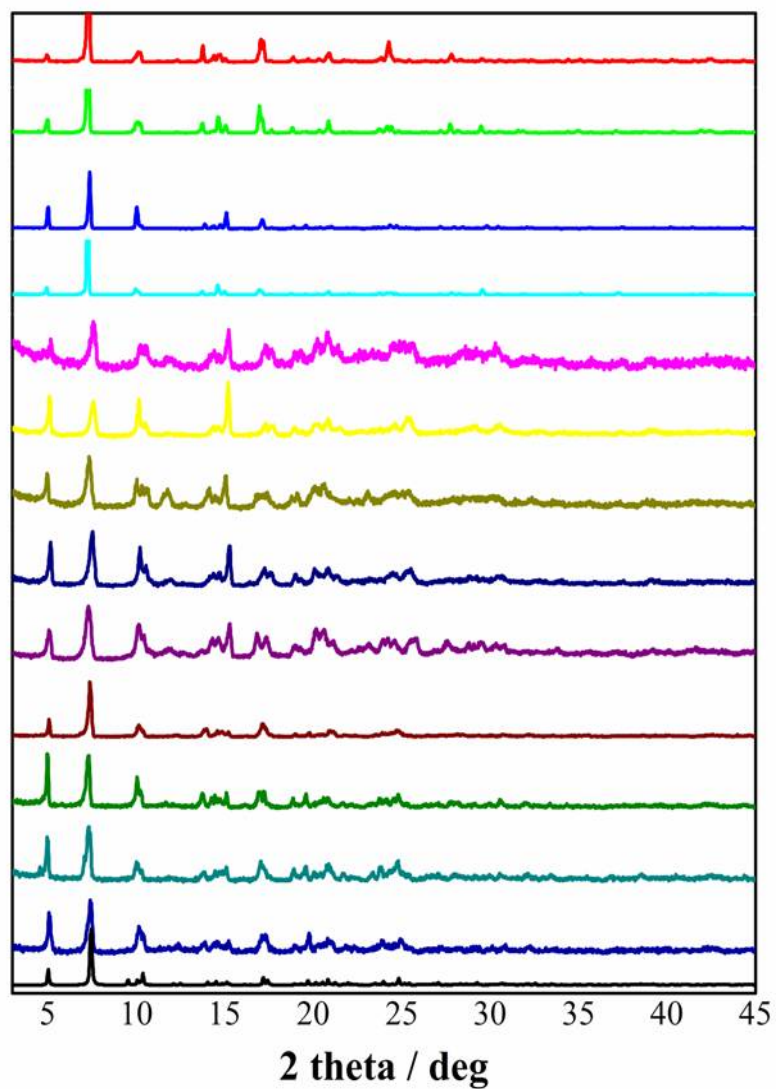


Fig. S4 The Powder X-ray diffraction pattern of **1** after sensing different solvents: simulated (black), DMAC (red), DMF (green), Tetrahydrofuran (THF) (blue), trichloromethane (cyan), acetone (magenta), acetonitrile (yellow), ethanol (dark yellow), ether (navy), dichloromethane (purple), isobutanol (wine), n-propanol (olive), methanol (dark cyan), and NB (royal).

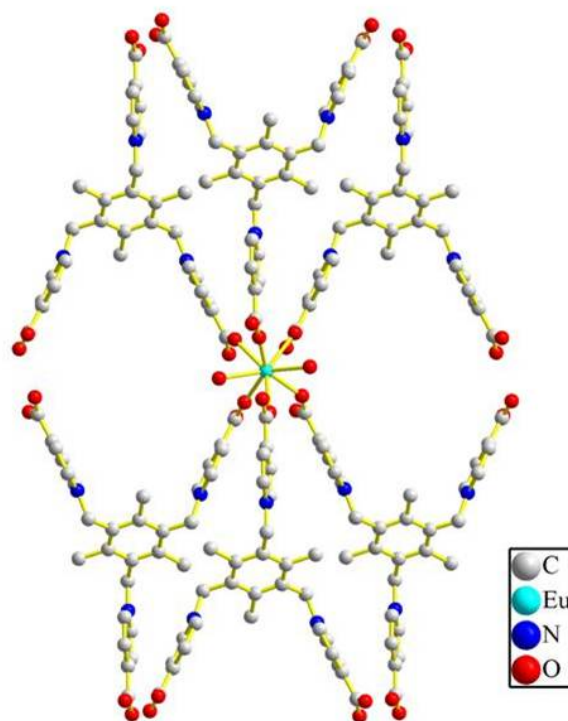


Fig. S5 The coordinated environment of Eu^{3+} ion in **1** (hydrogen atoms omitted for clarity).

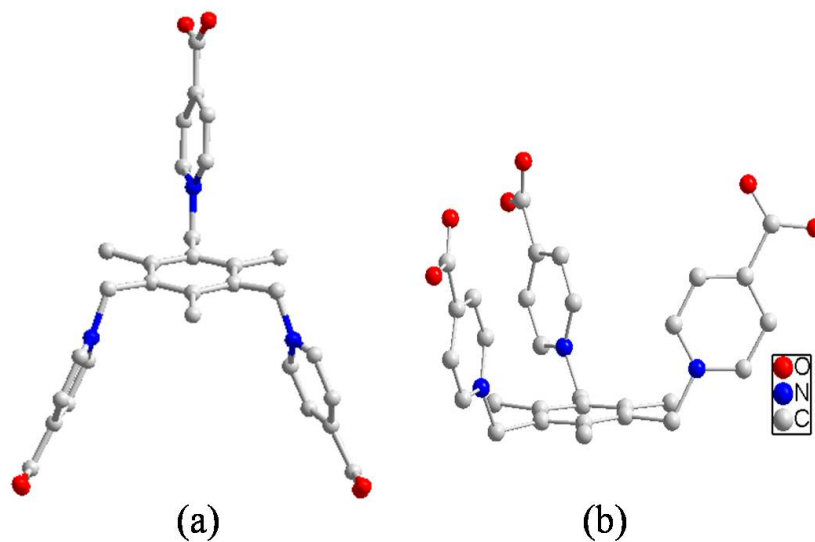


Fig. S6 (a) Chair-shaped configuration of **L** in compound **1**; (b) reported bowl-shaped configuration of **L**.¹

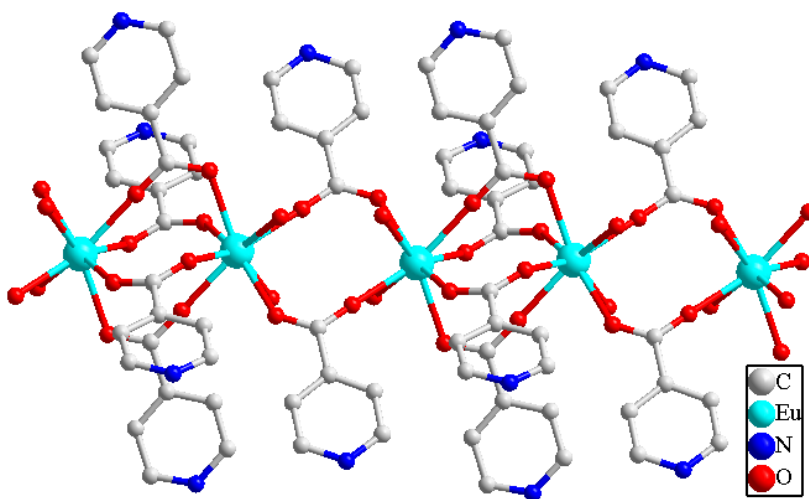


Fig. S7 1D infinite Eu(III) chain in **1**.

Luminescence Measurements

The fluorescence properties of **1** was investigated in the solid state and in various solvent suspensions at room temperature. The suspensions of **1** were prepared by introducing **1** powder (3 mg) into DMAC, DMF, THF, trichloromethane, acetone, acetonitrile, ethanol, ether, dichloromethane, isobutanol, n-propanol, methanol or NB solution (3.00 mL) at room temperature. Also, **1** and H_3LBr_3 were immersed in DMAC solutions containing the same concentrations of $\text{M}(\text{NO}_3)_x$ ($\text{M} = \text{Li}^+, \text{Na}^+, \text{K}^+, \text{Mg}^{2+}, \text{Ca}^{2+}, \text{Sr}^{2+}, \text{Al}^{3+}, \text{Cr}^{3+}, \text{Mn}^{2+}, \text{Fe}^{3+}, \text{Co}^{2+}, \text{Ni}^{2+}, \text{Cu}^{2+}, \text{Ag}^+, \text{Zn}^{2+}, \text{Cd}^{2+}, \text{Pb}^{2+}$), respectively. Samples were prepared by introducing **1** and H_3LBr_3 powder (3 mg) into DMAC solution (3.00 mL) at room temperature, respectively. Before photoluminescence measurements, the suspensions were oscillated for 10 min using ultrasonic waves to ensure uniform dispersion.

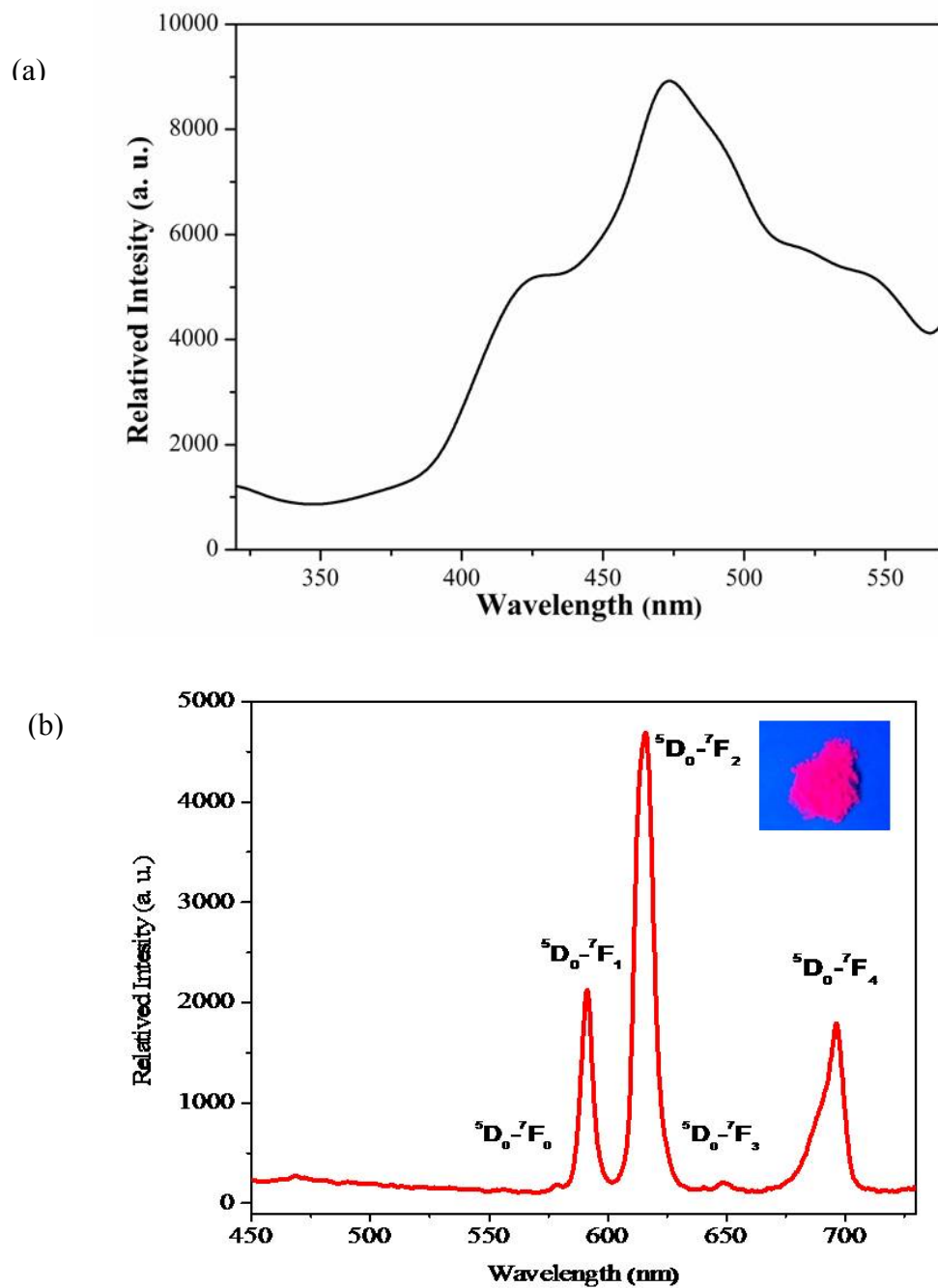


Fig. S8 (a) The solid-state emission spectra of free **L** ligands at room temperature ($\lambda_{\text{ex}} = 305$ nm); (b) The solid-state emission spectra of **1** at room temperature ($\lambda_{\text{ex}} = 375$ nm). The samples of **1** illuminated with 365 nm laboratory UV light are inserted.

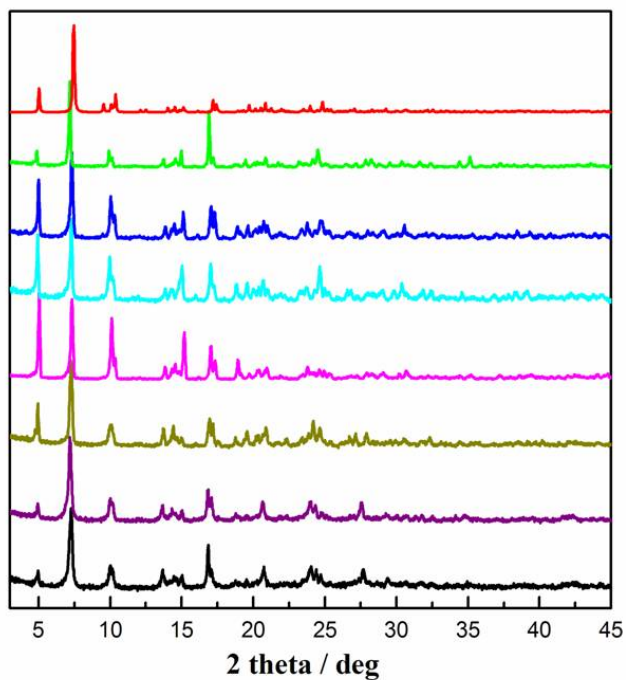


Fig. S9 The Powder X-ray diffraction pattern of **1** after sensing some representative metal ions: simulated (black), Na⁺ (red), Mg²⁺ (green), Al³⁺ (blue), Fe³⁺ (cyan), Co²⁺ (magenta), Cu²⁺ (dark yellow), and Zn²⁺ (purple).

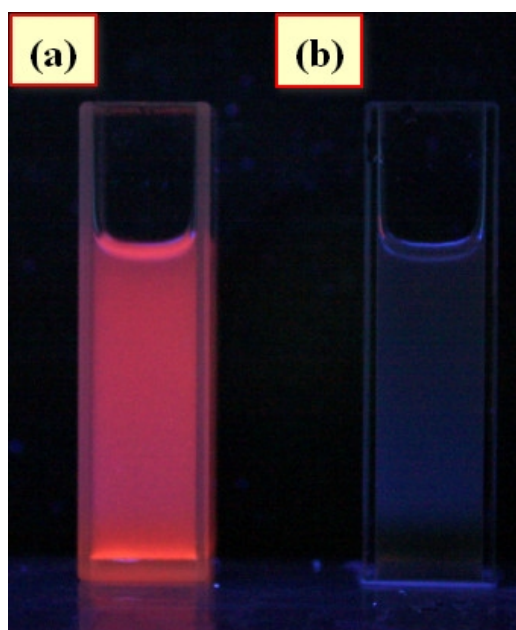


Fig. S10 (a) The naked-eye observation of **1** suspension without any metal ions showing red light under UV light; (b) The obviously luminescence quenching of **1** suspension containing Fe³⁺ under UV light.

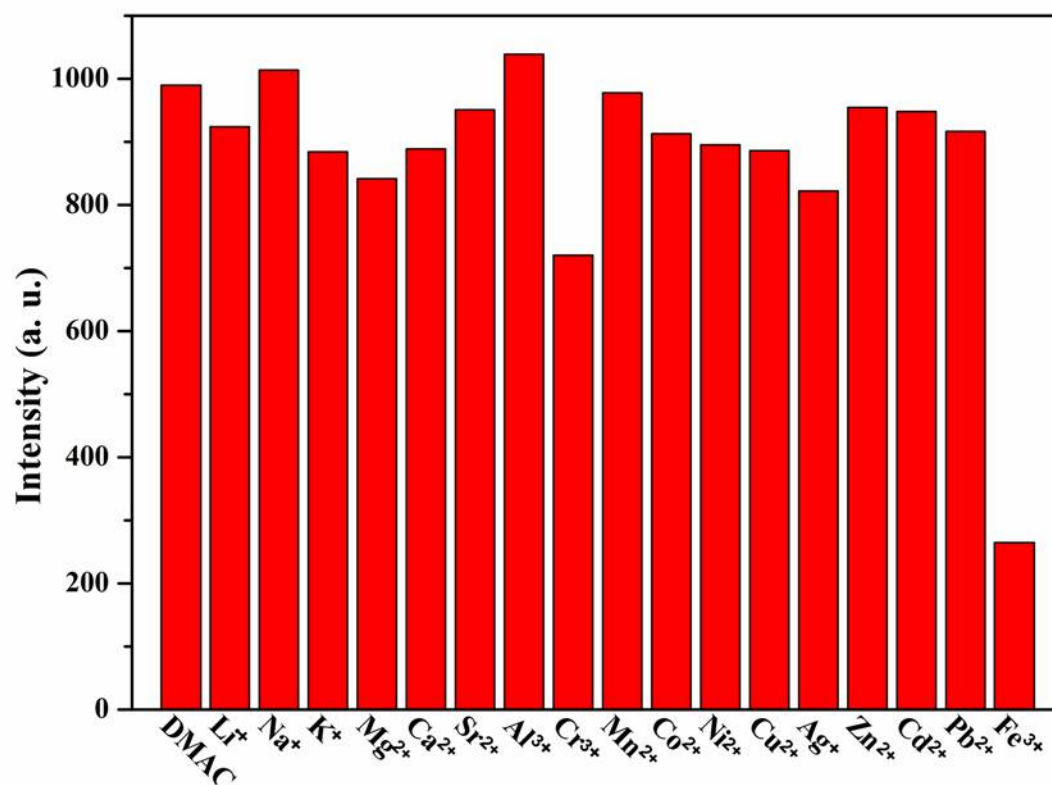


Fig. S11 The luminescent intensities for an emulsion of **L** in DMAC (10⁻³ M) at 473 nm upon the addition of various cations (excited at 305 nm).

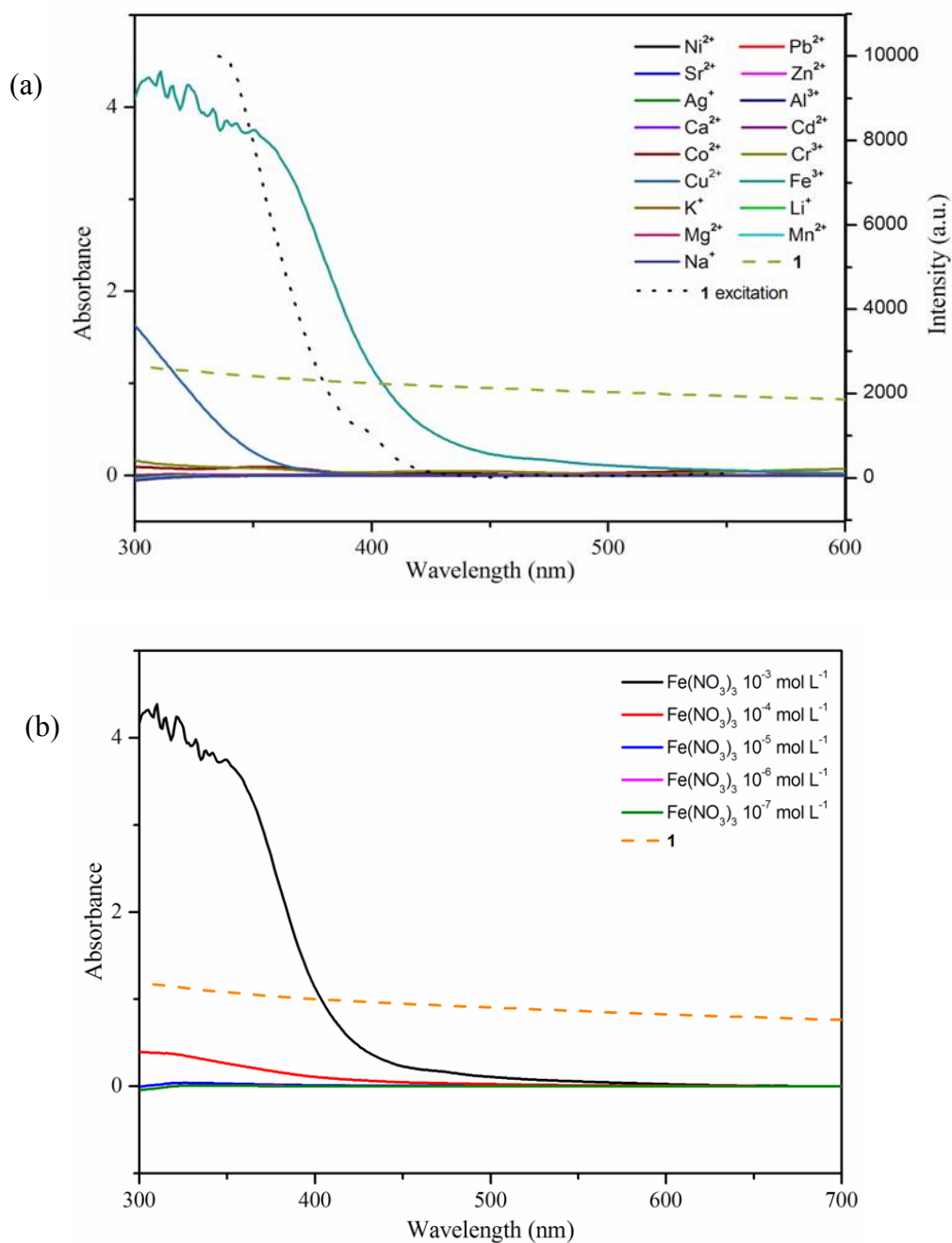


Fig. S12 (a) Solid line: UV-Vis spectra of DMAC solutions containing 10^{-3} M $M(\text{NO}_3)_x$ ($M = \text{Li}^+, \text{Na}^+, \text{K}^+, \text{Mg}^{2+}, \text{Ca}^{2+}, \text{Sr}^{2+}, \text{Al}^{3+}, \text{Cr}^{3+}, \text{Mn}^{2+}, \text{Fe}^{3+}, \text{Co}^{2+}, \text{Ni}^{2+}, \text{Cu}^{2+}, \text{Ag}^+, \text{Zn}^{2+}, \text{Cd}^{2+}, \text{Pb}^{2+}$); Dashed line: UV-Vis spectra of dispersed 3 mg **1** in 3 mL DMAC; Dotted line: Excitation ($\lambda_{\text{em}} = 618$ nm) spectra of dispersed 3 mg **1** in 3 mL DMAC; (b) Solid line: UV-Vis spectra of DMAC solutions containing different concentration of $\text{Fe}(\text{NO}_3)_3$; Dashed line: UV-Vis spectra of dispersed 3 mg **1** in 3 mL DMAC.

Table S3 The absorptive intensity of the DMAC solutions containing different concentration of Fe^{3+} at 375 nm and the luminescent intensity of **1** in the DMAC solutions containing different concentration of Fe^{3+} for the $^5\text{D}_0 \rightarrow ^7\text{F}_2$ transition (excited at 375 nm).

concentration of Fe^{3+}	absorptive intensity	luminescent intensity (a.u.)
0	0	2485
10^{-7}	0.003	2240.5
10^{-6}	0.004	2107.5
10^{-5}	0.02	1849.5
10^{-4}	0.176	735.25
10^{-3}	2.643	96.6

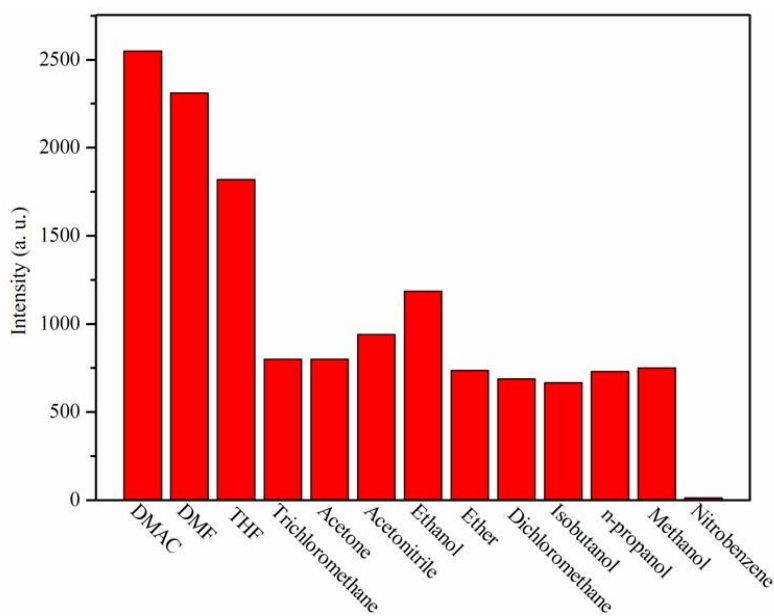


Fig. S13 The luminescence intensities of $^5\text{D}_0 \rightarrow ^7\text{F}_2$ transition for an emulsion of **1** in different solvents.

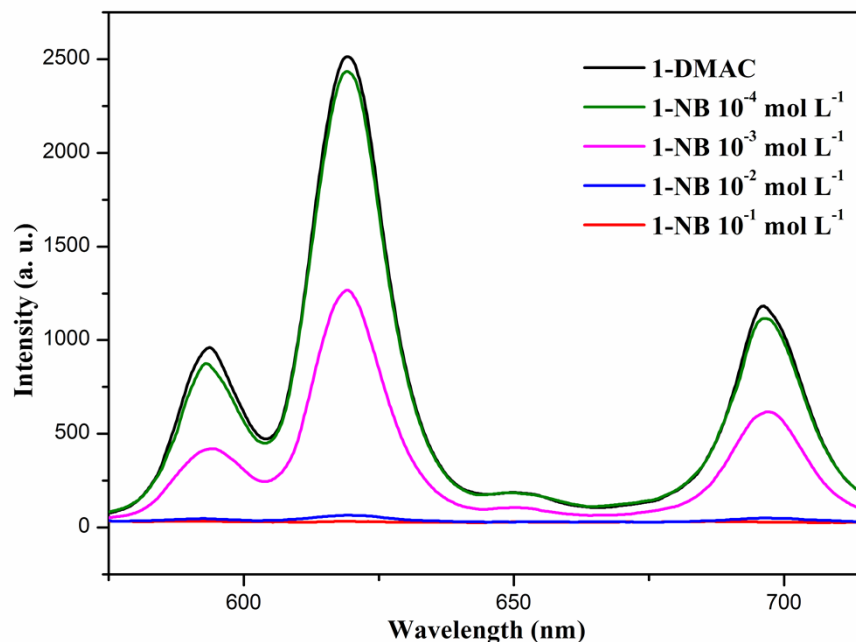


Fig. S14 The Fluorescence titration of **1** dispersed in DMAC with the addition of different concentrations of NB (excited at 375 nm)

Reference

1. G. Q. Kong and C. D. Wu, *Cryst. Growth Des.*, 2010, **10**, 4590.
2. (a) G. M. Sheldrick, *SHELXL97, Program for Crystal Structure Refinement*; University of Göttingen: Göttingen, Germany, 1997; (b) G. M. Sheldrick, *SHELXS97, Program for Crystal Structure Solution*; University of Göttingen: Göttingen, Germany, 1997.
3. A. L. Spek, *J. Appl. Crystallogr.*, 2003, **36**, 7.